

# Experimental Investigation of the Formation of Formaldehyde by Hadean and Noachian Impacts

Saeka Masuda,<sup>1</sup> Yoshihiro Furukawa,<sup>1</sup> Takamichi Kobayashi,<sup>2</sup> Toshimori Sekine,<sup>3,4</sup> and Takeshi Kakegawa<sup>1</sup>

## Abstract

Formaldehyde (FA) is an important precursor in the abiotic synthesis of major biomolecules including amino acids, sugars, and nucleobases. Thus, spontaneous formation of prebiotic FA must have been crucial for the chemical origin of life. The frequent impacts of meteorites and asteroids on Hadean Earth have been considered one of the abiotic synthetic processes of organic compounds. However, the impact-induced formation of FA from CO<sub>2</sub> as the major atmospheric constituent has not been confirmed yet. This study investigated the formation of FA in impact-induced reactions among meteoritic minerals, bicarbonate, gaseous nitrogen, and water to simulate the abiotic process experimentally. Products were analyzed with ultra-high-performance liquid chromatography/tandem mass spectrometry and powder X-ray diffraction techniques. The results show the formation of FA and oxidation of metallic iron to siderite in the impact shock experiments. This indicates that this important prebiotic molecule was also synthesized by impacts of iron-bearing meteorites/asteroids on the Hadean oceans. The impact events might have generated spatially and temporally FA-enriched localized environments. Moreover, the impact-induced synthesis of FA may have also occurred on Noachian Mars given the presence of liquid water and a CO<sub>2</sub>-N<sub>2</sub>-rich atmosphere on the planet. Key Words: Prebiotic formaldehyde—Meteorite impacts—Early Earth—Early Mars—Origin of life. *Astrobiology* 21, 413–420.

## 1. Introduction

**F**ORMALDEHYDE (FA) is an essential precursor in the abiotic synthesis of building blocks of life. For example, amino acids are formed by the reaction of FA, hydrogen cyanide, and ammonia in the Strecker synthesis (Harada, 1963) and by reacting FA and ammonia (Yanagawa *et al.*, 1980). Sugars, including ribose and glucose, are formed by polymerization of FA in alkaline solutions (Breslow, 1959; Kim *et al.*, 2011; Furukawa *et al.*, 2019). Sugars also form by impact-induced reactions from FA (Civiš *et al.*, 2016). Nucleobases form with formamide in impact-induced reactions from FA with molecular nitrogen (Ferus *et al.*, 2019). These previous explorations usually began with FA either delivered from space or already synthesized in early environments (Pinto *et al.*, 1980; Aponte *et al.*, 2019). Therefore, an evaluation of the *de novo* sources and sinks of FA in the early Earth environment is essential for understanding the processes involved in the prebiotic synthesis of building blocks of life.

Although a detailed composition of the Hadean atmosphere remains unclear, several authors postulate that the environment of Hadean Earth was neutral (*i.e.*, mostly CO<sub>2</sub> and N<sub>2</sub>) or slightly reduced, that is, containing a small amount of H<sub>2</sub> in addition to CO<sub>2</sub> and N<sub>2</sub> (Kasting, 1993; Tian *et al.*, 2005). Under such conditions, CO<sub>2</sub> might have been the major carbon source. This atmosphere might have been modified to more reduced compositions by the addition of reduced volatiles generated by impacts of extraterrestrial objects (Hashimoto *et al.*, 2007; Schaefer and Fegley, 2010; Furukawa *et al.*, 2014; Yang *et al.*, 2014), although the effects by the impact-generated volatiles to the global atmospheric composition remain unclear.

Sources of FA on Hadean Earth may have included the following: (1) photochemical reactions between CO<sub>2</sub> and H<sub>2</sub>O (Pinto *et al.*, 1980; Holland, 1984); (2) formation during an electric discharge, for instance in CO- and CH<sub>4</sub>-rich atmospheres, or CO<sub>2</sub>-based atmospheres that were saturated with H<sub>2</sub> (Miller, 1953); and (3) direct input from extraterrestrial sources (Aponte *et al.*, 2019).

<sup>1</sup>Department of Earth Science, Tohoku University, Sendai, Japan.

<sup>2</sup>National Institute for Materials Science, Tsukuba, Japan.

<sup>3</sup>Center for High Pressure Science & Technology Advanced Research, Shanghai, China.

<sup>4</sup>Graduate School of Engineering, Osaka University, Osaka, Japan.

Based on the lunar crater records and the content of highly siderophile elements in Earth's mantle, the flux of extraterrestrial objects to Hadean Earth may have been significantly high (Hartmann *et al.*, 2000; Valley *et al.*, 2002; Day *et al.*, 2016). Additionally, compared to other energy sources, such as ultraviolet radiation and lightning, the available energy due to impacts on Hadean Earth would have been significant (Chyba and Sagan, 1992). Many experimental and theoretical simulations have suggested an impact-induced formation of reduced species of inorganic compounds (Sugita and Schultz, 2003; Schaefer and Fegley, 2010; Kurosawa *et al.*, 2013; Furukawa *et al.*, 2014). Consequently, the formation of the building blocks of life from inorganic compounds by impacts of iron-bearing meteorites was proposed (Nakazawa *et al.*, 2005; Nakazawa, 2018), and subsequent experimental simulations demonstrated the formation of various organic compounds including amino acids (Furukawa *et al.*, 2009, 2015). Additionally, large impactors tend to contain higher amounts of metallic iron that potentially works as a reductant and a catalyst (Pasek and Lauretta, 2008). Catalytic behavior of minerals in carbonaceous chondrites in the synthesis of organic acids, nucleobases, and amino acids from formamide and water has been reported (Rotelli *et al.*, 2016). Laboratory simulation studies of the hypervelocity impact of meteorites by using laser-pulse heating of an ordinary chondrite have reported the formation of various gaseous molecules including acetaldehyde (Mukhin *et al.*, 1989). These studies suggest the formation of FA during hypervelocity impacts on CO<sub>2</sub> and H<sub>2</sub>O that are regarded as the major C and H forms on Hadean Earth (Abe and Matsui, 1988; Kasting, 1990; Trail *et al.*, 2011). Formation of RNA components from organic compounds including FA by impacts has also been discussed as the origin of RNA components (Ferus *et al.*, 2015, 2017, 2019; Benner *et al.*, 2020). However, synthesis of FA via impacts from CO<sub>2</sub> remained unclear. The present study investigates the FA synthesis in impact-induced reactions that are considered to have occurred on Hadean Earth during impacts of chondritic asteroids/meteorites.

## 2. Experimental

### 2.1. Materials

Mg<sub>2</sub>SiO<sub>4</sub>, a natural forsterite from Myanmar, was used as the starting material after it was washed, crushed, and heated at 450°C in air for 6 h. Iron (99.9 % wt, powder <45 μm in diameter), nickel (99.95 % wt, sponge), and magnetite (>95%) were from Wako (Osaka, Japan). <sup>13</sup>C-labeled amorphous carbon (97 wt %, 99% <sup>13</sup>C, amorphous) was from Cambridge Isotope Laboratories (Tewksbury, USA). This carbon was further heated at 500°C for 6 h in air before use. <sup>13</sup>C-labeled sodium bicarbonate (<sup>13</sup>C, 99%) was obtained from Cambridge Isotope Laboratories. Ammonia used in the experiment was from Aldrich (28% NH<sub>3</sub> in double distilled water, PPB/PTFE grade). The absence of the contamination of glycine and alanine in this ammonia solution was confirmed with liquid chromatography/tandem mass spectrometry. Acetonitrile (LC-MS grade) that was used as a chromatography eluent was from Kanto (Tokyo, Japan). Commercial FA-2,4-DNPH from Sigma-Aldrich was used as the referential standard for mass spectrometry and chromatography. The water was purified with a Milli-Q

Integral MT (TOC: <5 ppm, 18.2 MΩcm). The absence of FA in the purified water was confirmed by the same analysis as the samples. Pure nitrogen gas (>99.995%) was used to fill the open space of the sample cavity. All glassware was heated at 450°C in air for 6 h before use. The design of the shock-recovery experiments, including the sample container and flyer, was described in the work of Furukawa *et al.* (2007). The sample container was washed with purified water, methanol, and hexane (methanol and hexane, grade 5000 for pesticide residue and PCB analysis; Wako) and completely dried.

### 2.2. Methods

A series of shock-recovery experiments were conducted by using a single-stage propellant gun at the National Institute for Materials Science, Japan, to simulate the impact-induced reactions generated by impacts of different types of chondritic asteroids/meteorites on NH<sub>3</sub>-free and NH<sub>3</sub>-containing oceans covered by an N<sub>2</sub>-CO<sub>2</sub> atmosphere (Sekine, 1997). The starting materials were composed of mixtures of minerals, fluids (water or ammonia water), and <sup>13</sup>C-labeled sodium bicarbonate, and N<sub>2</sub> gas was used to fill up the sample cavity (Table 1). When all the NaHCO<sub>3</sub> decomposes into CO<sub>2</sub>, the atmosphere in the sample becomes very CO<sub>2</sub>-rich; molar mixing ratios of CO<sub>2</sub>/N<sub>2</sub> are 118 or 176. The sample container and geometry were described in the work of Furukawa *et al.* (2007). Three types of mineral mixtures were used as analogs of chondritic asteroids/meteorites: an iron meteorite type (IM), an ordinary chondrite type (OC), and a carbonaceous chondrite type (CC). IM, OC, and CC analogs were prepared from a mixture of metallic iron and nickel; a mixture of forsterite (Mg<sub>2</sub>SiO<sub>4</sub>), metallic iron, and nickel; and a mixture of forsterite, magnetite (Fe<sub>3</sub>O<sub>4</sub>), amorphous carbon, metallic iron, and metallic nickel, respectively. The iron content in the meteorite analogs of IM, OC, and CC was 91, 32, and 14 wt %, respectively. These values are somewhat higher than the typical content of metallic iron in iron meteorite, ordinary chondrite (H chondrite), and carbonaceous chondrite (*i.e.*, >80 wt %, 0–26 wt % [mostly more than 10 wt %], and 0–13 wt %, respectively) (Mittlefehldt *et al.*, 1998; Kimura *et al.*, 2018). The impacts were conducted at close to the same impact velocities, approximately 0.9 km/s. The impact generated a shockwave of approximately 7 GPa and an in-shock temperature of approximately 300°C for 0.7 μs. Post-shock temperature was estimated to be approximately 1500°C (Furukawa *et al.*, 2011).

Static heating experiments were also conducted in tandem at 150°C for 6 h in an electric furnace for comparison. The design of the static heating experiments, including the sample container, reagents, and analytical methods, was analogous to that of the shock-recovery experiments except for the heat source. A control shock experiment that did not contain <sup>13</sup>C-labeled sodium bicarbonate (No. 27) in the starting material was also conducted for comparison.

The sample container was trimmed and washed with purified water, methanol, and hexane. The container was then cooled with liquid nitrogen to freeze the volatile samples in the cavity. Then two extraction holes were made through the wall of the sample cavity. The sample container was soaked in pure water; then the product FA was extracted

TABLE 1. AMOUNTS OF STARTING MATERIALS, PRODUCTS, AND EXPERIMENTAL CONDITIONS

| No. | ID      | Starting materials |                                     |         |                                       |                              |  |                      |                       |                       |                        | Exp. condition    |                    |                    |                                  |                            | Product (nmol)             |                                    |  |
|-----|---------|--------------------|-------------------------------------|---------|---------------------------------------|------------------------------|--|----------------------|-----------------------|-----------------------|------------------------|-------------------|--------------------|--------------------|----------------------------------|----------------------------|----------------------------|------------------------------------|--|
|     |         | Fe (mg)            | Fe <sub>3</sub> O <sub>4</sub> (mg) | Ni (mg) | Mg <sub>2</sub> SiO <sub>4</sub> (mg) | Amorph. <sup>13</sup> C (mg) | NaH <sup>13</sup> CO <sub>3</sub> (mg) | NH <sub>3</sub> (mg) | H <sub>2</sub> O (mg) | N <sub>2</sub> (μmol) | Impact velocity (km/s) | 150°C heating (h) | <sup>13</sup> C-FA | <sup>12</sup> C-FA | <sup>13</sup> C/ <sup>12</sup> C | Contam. <sup>13</sup> C-FA | Product <sup>13</sup> C-FA | Product <sup>13</sup> C-FA average |  |
| 21  | IM1     | 300                | 0                                   | 30      | 0                                     | 0                            | 0                                      | 130                  | 20                    | 0.92                  | -                      | 1.4               | 10.9               | 0.132              | 0.2                              | 1.2                        | 2.5 ± 1.4                  |                                    |  |
| 22  |         | 300                | 0                                   | 30      | 0                                     | 0                            | 0                                      | 130                  | 20                    | 0.92                  | -                      | 4.1               | 60.3               | 0.068              | 1.1                              | 2.9                        |                            |                                    |  |
| 23  |         | 300                | 0                                   | 30      | 0                                     | 0                            | 0                                      | 130                  | 20                    | 0.95                  | -                      | 4.4               | 49.9               | 0.089              | 0.9                              | 3.5                        |                            |                                    |  |
| 25  | IM2     | 300                | 0                                   | 30      | 0                                     | 0                            | 0                                      | 130                  | 20                    | 0.94                  | -                      | 3.5               | 13.6               | 0.258              | 0.3                              | 3.2                        | 2.2 ± 1.0                  |                                    |  |
| 26  |         | 300                | 0                                   | 30      | 0                                     | 0                            | 0                                      | 130                  | 20                    | 0.85                  | -                      | 1.3               | 5.2                | 0.251              | 0.1                              | 1.2                        |                            |                                    |  |
| 27  | IM-cont | 300                | 0                                   | 30      | 0                                     | 0                            | 0                                      | 130                  | 20                    | 0.88                  | -                      | 0.1               | 5.5                | <b>0.019</b>       | 0.1                              | 0                          | 0                          |                                    |  |
| 28  | OC      | 100                | 0                                   | 10      | 0                                     | 0                            | 0                                      | 130                  | 20                    | 0.93                  | -                      | 1.5               | 14.7               | 0.102              | 0.3                              | 1.2                        | 2.1 ± 1.1                  |                                    |  |
| 29  |         | 100                | 0                                   | 10      | 0                                     | 0                            | 0                                      | 130                  | 20                    | 0.96                  | -                      | 3.7               | 33.7               | 0.110              | 0.6                              | 3.1                        |                            |                                    |  |
| 30  | CC      | 25                 | 50                                  | 8       | 15                                    | 0                            | 0                                      | 130                  | 20                    | 0.92                  | -                      | 3.4               | 37.4               | 0.092              | 0.7                              | 2.7                        | 3.0 ± 1.7                  |                                    |  |
| 31  |         | 25                 | 50                                  | 8       | 15                                    | 0                            | 0                                      | 130                  | 20                    | 0.87                  | -                      | 4.4               | 65.9               | 0.067              | 1.3                              | 3.2                        |                            |                                    |  |
| 43  | OC_Sta  | 100                | 0                                   | 10      | 0                                     | 0                            | 0                                      | 130                  | 20                    | -                     | 6                      | 0.6               | 34.3               | 0.017              | 0.7                              | -0.1                       | -0.1 ± 0.3                 |                                    |  |
| 44  | CC_Sta  | 25                 | 50                                  | 8       | 15                                    | 0                            | 0                                      | 130                  | 20                    | -                     | 6                      | 0.2               | 14.5               | 0.016              | 0.3                              | 0.0                        | 0.0 ± 0.1                  |                                    |  |
| 45  | IM_Sta  | 300                | 0                                   | 30      | 0                                     | 0                            | 0                                      | 130                  | 20                    | -                     | 6                      | 0.1               | 6.4                | 0.015              | 0.1                              | 0.0                        | -0.1 ± 0.1                 |                                    |  |
| 46  |         | 300                | 0                                   | 30      | 0                                     | 0                            | 0                                      | 130                  | 20                    | -                     | 6                      | 0.2               | 14.5               | 0.013              | 0.3                              | -0.1                       |                            |                                    |  |

through the sample holes. Solid residues were collected from the sample container and dried under vacuum for powder X-ray diffraction (XRD) analysis.

The concentration of FA in the extracted solution was determined with ultra-high-performance liquid chromatography/tandem mass spectrometry (UHPLC/MSMS; Shimadzu LCMS-8040) after derivatization with 2,4-dinitrophenylhydrazine (DNPH). The DNPH derivatization was conducted for 20 min at room temperature (~20°C) in a stirred mixture containing 20 μL of 17% phosphoric acid solution and 50 μL of 1 mg/mL DNPH in acetonitrile (99.9%; GL Science). UHPLC/MSMS was conducted with a reversed-phase column (Waters BEH C18; 2.1 mm I.D., 100 mm length, 1.7 μm particles) and an eluent (water-acetonitrile, 60/40 [v/v]). The column temperature and the flow rate were 35°C and 0.5 mL/min, respectively. The <sup>12</sup>C-FA and <sup>13</sup>C-FA were measured with multiple reaction monitoring (MRM) mode. In the MRM mode, the signal of a fragment ion (*m/z*: 151) that is produced by the fragmentation of a precursor ion (*m/z*: 209 for derivatized <sup>12</sup>C-FA and 210 for derivatized <sup>13</sup>C-FA) is monitored. Nebulizer flow, desolvation temperature, and heat block temperature were set at 2.8 L/min, 250°C, and 400°C, respectively. Powder XRD measurements by Philips PW3050 were conducted with reflection-free sample holders as described in the work of Furukawa *et al.* (2011).

### 3. Results

Figure 1 summarizes the results of the UHPLC/MSMS analysis. Both <sup>12</sup>C-FA and <sup>13</sup>C-FA were detected in all samples including those from the control experiment in which the <sup>13</sup>C-labeled carbon source was not added initially (Fig. 1d). This observation is plausible when biogenic FA is contaminated in the process of analysis since <sup>13</sup>C is present in biogenic FA at approximately 1:99 (wt/wt) of the amount of <sup>12</sup>C (Fig. 1). The actual ratio of <sup>13</sup>C-FA (*m/z*: 210 > 151) to <sup>12</sup>C-FA (*m/z*: 209 > 151) was determined experimentally at 0.019 by using a derivatized control sample that did not contain any <sup>13</sup>C-labeled carbon source (Table 1). As shown in Fig. 1, the <sup>13</sup>C-FA/<sup>12</sup>C-FA ratios of experimental products are significantly higher than those from control samples and standards. The amounts of <sup>13</sup>C-FA in products were determined via subtraction of the contaminant <sup>13</sup>C-FA, which was calculated using the amount of <sup>12</sup>C-FA and the referential ratio of <sup>13</sup>C-FA/<sup>12</sup>C-FA of the <sup>13</sup>C-free control experiment (Table 1; Fig. 2).

The amounts of <sup>13</sup>C-FA in the products clearly indicate the formation of FA in experiments that were subjected to a shock wave (IM1, IM2, OC, and CC in Fig. 2). The <sup>13</sup>C-FA production was negligible in both static heating experiments conducted at 150°C in place of shock heating (IM\_Sta in Fig. 2 and No. 43–46 in Table 1). The difference in the amounts of <sup>13</sup>C-FA produced from experiments using different meteorite analogs was within the experimental reproducibility (Fig. 2; CC, OC, IM1, and IM2). The yield of FA per mole of carbon dioxide was 8.5 × 10<sup>-5</sup> to 1.3 × 10<sup>-4</sup> mol % (Table 1). The presence of ammonia had a negligible effect on FA yields.

The results of powder XRD analysis on product residues are shown in Fig. 3. In all the shock experiments, metallic iron was partially oxidized to form siderite (FeCO<sub>3</sub>) (Fig. 3a, 3b). In contrast, siderite and magnetite (Fe<sub>3</sub>O<sub>4</sub>)

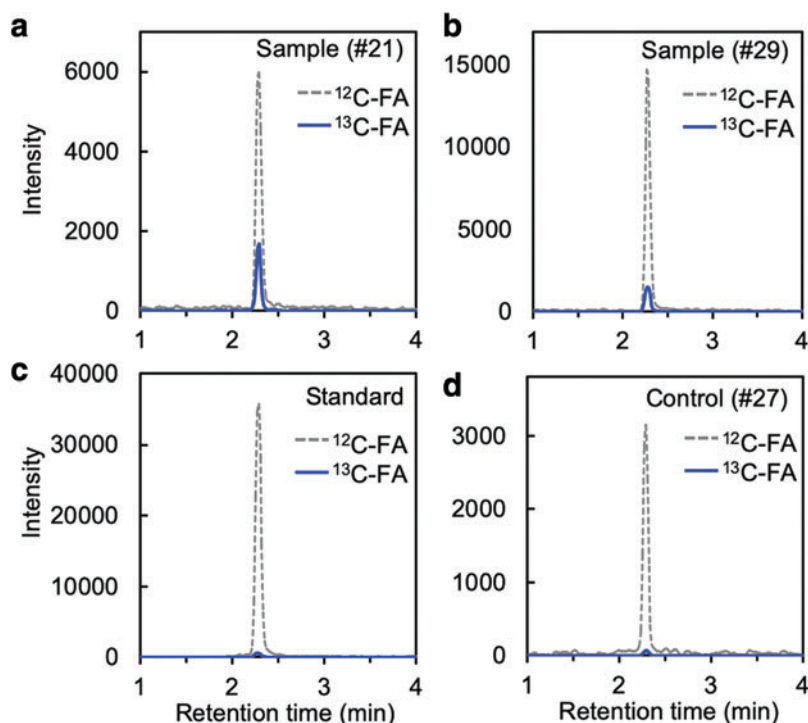


**FIG. 1.** Mass chromatograms of FA in the products, the control sample, and a commercial FA-2,4-DNPH standard. Multiple reaction monitoring (MRM) chromatograms of  $m/z$ : 209 > 151 and  $m/z$ : 210 > 151 are shown as  $^{12}\text{C}$ -FA and  $^{13}\text{C}$ -FA, respectively. The control (#27), sample #21, and sample #29 are the experiment without  $\text{NaH}^{13}\text{CO}_3$ , the experiment using ordinary chondrite analog (OC), and the experiment using iron meteorite analog without ammonia (IM1), respectively. Color images are available online.

were formed in the static heating experiments, but FA was not formed (Figs. 2 and 3c). Ni remained in all experimental products. The effect of ammonia was negligible on the production of the post-shock minerals (Fig. 3a, 3b).

## 4. Discussion

### 4.1. FA formation in impact-induced reactions

Although  $\text{NaHCO}_3$  is highly soluble in water, the low water quantity (*i.e.*, 130 mg) in the experimental setup en-

sured that, at most, 7% of  $\text{NaHCO}_3$  in the starting materials dissolved in water as  $\text{Na}^+$  and  $\text{HCO}_3^-$ . The remaining  $\text{NaHCO}_3$  was thermally decomposed into  $\text{CO}_2$ ,  $\text{H}_2\text{O}$ , and  $\text{Na}_2\text{CO}_3$  during the shock and static heating.

Powder XRD results indicate that iron was partially oxidized to  $\text{Fe}^{2+}$  by both the shock and static heating procedures (Fig. 3b). The oxidation of iron by  $\text{H}_2\text{O}$  generally indicates the formation of reductant, that is,  $\text{H}_2$ . However, a theoretical study has suggested the formation of H atoms on the surface of iron during shock compression (Shimamura *et al.*, 2016).

The formation of FA indicates that bicarbonate or  $\text{CO}_2$  was reduced during the experiment. Indeed, high-yield catalytic reduction of  $\text{CO}_2$  to FA and methanol has been reported in industrial applications (Idriss *et al.*, 1996; Bontempo *et al.*, 2014). In the present experiments, FA was strictly formed in the experiments with shock heating, although iron was oxidized in experiments with both shock and static heating. This indicates that  $\text{CO}_2$  or  $\text{HCO}_3^-$  reduction followed different pathways in the shock and static heating procedures. An *ab initio* molecular dynamics study suggested that, within picoseconds and in the presence of  $\text{CO}_2$ ,  $\text{H}_2\text{O}$ , and Fe, multistep reactions on the surface of Fe lead to the formation of formic acid ( $\text{HCOOH}$ ) via CO and  $\text{HCO}_3^-$  (Shimamura *et al.*, 2019). This simulation also shows that  $\text{HCOOH}$  generation from  $\text{HCO}_3^-$  depends on the shock pressure, which promotes the formation of H atoms on the Fe surface. This pressure effect could have resulted in the formation of FA exclusively in the shock experiments. It is also possible that, due to longer reaction durations in the present experiments than the numerical simulation, hydrogen atoms on the Fe surface further reduced formic acid or its precursor.

Oxidation of iron could be one of the steps in the formation of organic compounds, including FA, during impact.

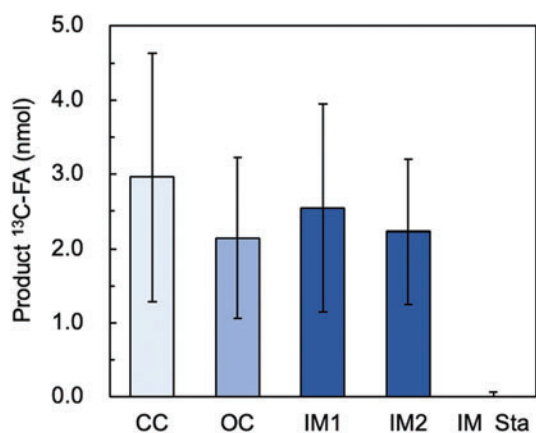


**FIG. 2.** Amounts of product  $^{13}\text{C}$ -FA. The error bar in IM1 indicates  $1\sigma$  for triplicate values while error bars in OC, CC, IM2, and IM\_Sta experiments are a percent error of IM1. OC, CC, IM2, and IM\_Sta represent experiments using analogous materials of ordinary chondrite, carbonaceous chondrite, iron meteorite, and iron meteorite with static heating, respectively. The details are listed in Table 1. Color images are available online.

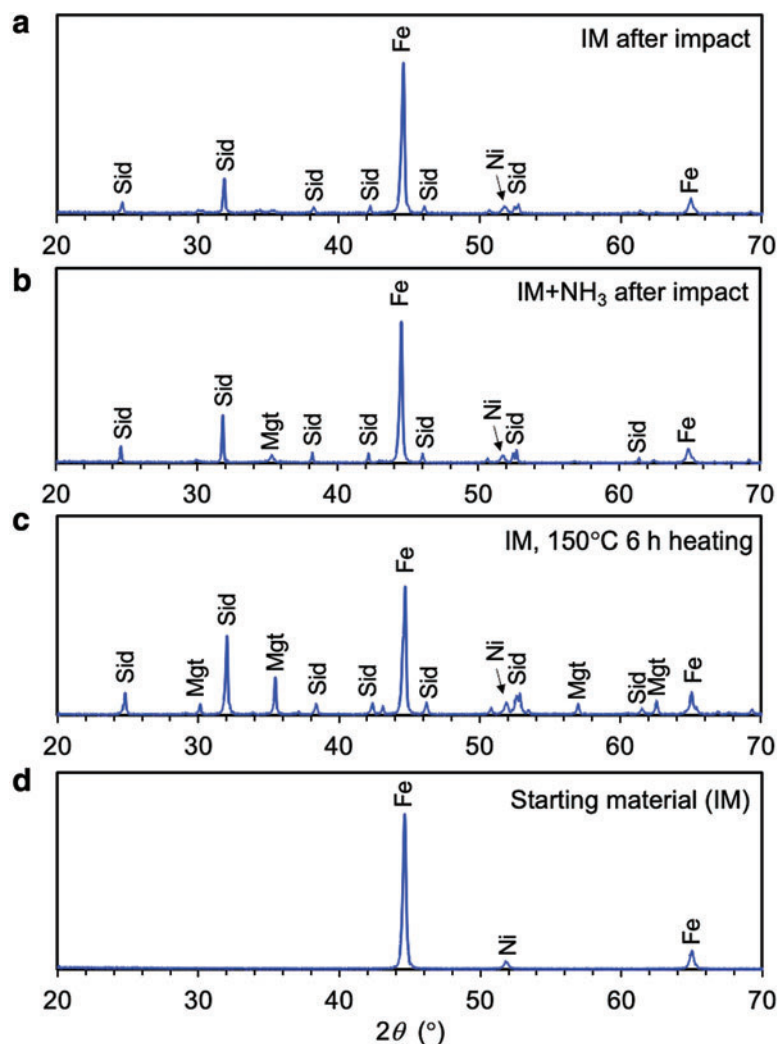


**FIG. 3.** Powder XRD profiles of starting materials and product residues. Sid=siderite ( $\text{FeCO}_3$ ); Mgt=magnetite ( $\text{Fe}_3\text{O}_4$ ). (a) Iron meteorite analog (IM) experiment after impact (#21). (b) Iron meteorite analog experiment with ammonia after impact (#25). (c) Experiment using iron meteorite analog after static heating (#45). (d) Iron meteorite analog (*i.e.*, starting material). Color images are available online.

However, the amounts of consumed metallic Fe were not significantly different between the experiments probably due to the limited exposure duration to the shock heating. This similarity in the extent of Fe consumption may have caused a similarity in the extent of the reduction of  $\text{HCO}_3^-$  to formic acid and FA in experiments with different meteorite analogs. Many reactions including the formation of amino acids, amines, and carboxylic acids may have proceeded simultaneously after the formation of FA. In previous studies, ammonia has been found to react with FA and result in the formation of various molecules such as amines and amino acids (Furukawa *et al.*, 2015). However, the lower yields of amino acids found in a previous study suggest a negligible consumption of FA during the reaction (Takeuchi *et al.*, 2020). The negligible differences in FA yields between the experiments with and without ammonia imply that the rates and extent of other FA-consuming reactions were low.

#### 4.2. Implication to natural impacts

In natural meteorite/asteroid impacts, large projectiles more than 100m in diameter collide with Earth at hypervelocities that exceed 10km/s (Hills and Goda, 1993). Smaller-sized (less than 20m) asteroids or meteorites have

low impact velocities due to deceleration in the atmosphere (Hills and Goda, 1993). Impact velocities can vary from very low to 10 km/s for projectiles with an initial size of 20–100 m (Hills and Goda, 1993). Some of the conditions inherent in middle-sized natural projectile impacts correspond to the present experimental conditions. However, the duration of exposure to elevated temperature and pressure was significantly lower in the experiments. Furthermore, even during single impact, the pressure and temperature of fragments after the impact differ significantly depending on the location in the impact plume (Pierazzo and Chyba, 1999).

The presence of substantial relicts of metallic iron in the experimental products indicates that the reactions have significant potential for further FA production and were only limited by the extremely short duration ( $< 1 \mu\text{s}$ ) of shock heating. In the natural hypervelocity impacts of asteroids/meteorites, shock durations are typically several orders of magnitude longer and shock compression and heating are more significant than in the present experimental conditions (*e.g.*, more than  $10^3$  K, 100 GPa, and 0.1 s) (Hills and Goda, 1993; Pierazzo and Chyba, 1999; Pierazzo and Melosh, 2000). Therefore, higher FA yields are expected due to significant iron oxidation and hydrogen production by large projectiles with high impact velocities. A previous calculation

also indicates the positive correlation between the impact velocity and formic acid yields (Shimamura *et al.*, 2019).

The conversion rate of carbon to FA was at least  $9 \times 10^{-5}$  mol % in OC analog experiments. The production rate of FA from Fe was  $1.3 \times 10^{-4}$  mol %, assuming that 30% of iron was consumed during the experiments. Previous studies suggest that huge amounts of extraterrestrial objects,  $\sim 4 \times 10^{23}$  g, accreted the Hadean Earth in the Late Heavy Bombardment (LHB) (Anders, 1989). Assuming that ordinary chondrite with typical 10 wt % metallic iron, that is,  $\sim 4 \times 10^{22}$  g Fe, accreted during the LHB period, then the yields from the present experiments and the iron flux predict the production of  $\sim 9 \times 10^{16}$  mol of FA during the LHB. However, this estimate may only be a baseline value since higher temperatures and pressures, as well as longer reaction durations, may provide much higher yields. The actual amount of FA that was produced by natural impacts on Hadean Earth is presently unclear because local time-dependent, pressure-temperature conditions in natural hypervelocity impacts have significant variations.

The yields of FA in the present experiments were approximately one order of magnitude higher than the yields of amino acids formed in similar impact conditions (Takeuchi *et al.*, 2020). This suggests that FA may be a precursor in the formation of amino acids during impact-induced synthesis. Additionally, FA that was formed by impacts on Hadean Earth might have contributed in formation of the building blocks of life through other reactions such as sugar formation by the formose reaction (Breslow, 1959; Kim *et al.*, 2011; Civiš *et al.*, 2016; Furukawa *et al.*, 2019).

Photochemical reaction is a traditional model that has been used to explain the source of Hadean FA. Pinto *et al.* (1980) estimated that the FA produced by photochemical reactions corresponds to a concentration of  $10^{-3}$  M in oceans at the current volume with a  $N_2$ - $CO_2$ -dominated atmosphere, given  $10^7$  years of accumulation. The total amount of FA produced during impacts does not exceed that generated in photochemical reactions since the concentration of FA in oceans, at the present water volume, is estimated by the baseline impact synthesis (*i.e.*,  $\sim 9 \times 10^{16}$  mol) to be  $\sim 7 \times 10^{-5}$  M. Nevertheless, the impact-induced synthesis might have resulted in a spatially and temporally localized FA-enrichment that could have exceeded the global average concentration generated by photochemical reactions. High concentration of FA (*e.g.*,  $10^{-3}$  M) is one of the most important requirements for the formation of life's building molecules (Cleaves, 2008). Therefore, the impact-induced FA formation might have contributed to the chemical evolution of the ingredients of prebiotic molecules on Hadean Earth.

#### 4.3. Potential FA formation on Noachian Mars

Formaldehyde was tentatively detected in the martian atmosphere more than 25 years ago (Korablev *et al.*, 1993). It has sometimes been debated as the product of  $CH_4$  oxidation and thus regarded as a potential sign of martian life (Weiss *et al.*, 2000; Summers *et al.*, 2002). However, the actual presence of FA on ancient and present Mars remains unclear.

Significant crater density on the southern hemisphere of Mars indicates that impacts of meteorites/asteroids were frequent on Noachian Mars (Hartmann and Neukum, 2001;

Carr and Head, 2010). A great deal of geological evidence, including the valley network found by a martian orbiter and sedimentary structures found by martian rovers, suggests the presence of liquid surface water on Noachian Mars (Head *et al.*, 1999; Fairén *et al.*, 2003; Squyres *et al.*, 2004; Di Achille and Hynek, 2010). Furthermore, the presence of redox-sensitive minerals in martian meteorites suggests that degassed species produced by martian volcanic activity were composed of  $CO_2$  with small amounts of CO and  $CH_4$  (Schmidt *et al.*, 2013). The atmosphere was also influenced by the degassed species escaping to space. The overall atmospheric composition of Noachian Mars remains unclear, but a numerical simulation suggests a  $CO_2$ - $N_2$ -rich atmosphere with reduced species (Batalha *et al.*, 2015). The presence of carbonates in Noachian sediments also supports a  $CO_2$ -dominated atmosphere (Ehlmann *et al.*, 2008).

The results of the present study suggest that impacts of Fe-bearing meteorite/asteroids on the Noachian ocean formed FA from  $CO_2$ , which might have been a major, though rather unreactive, carbon source. Other FA formation processes on Noachian Mars remain unclear, but photochemically induced FA synthesis might have been possible. The ancient martian FA produced by impacts may have been utilized in many reactions and decomposition processes and potentially used in the synthesis of life's building blocks. Direct synthesis of amino acids by impact-induced reactions has also been recently suggested (Takeuchi *et al.*, 2020). The organic compounds once formed by such events on Noachian Mars might have been oxidized in the subsequent environmental changes on the surface of Hesperian Mars (Benner *et al.*, 2000).

## 5. Conclusion

We have shown by laboratory simulation that FA can be formed via impact-induced reactions between major meteorite minerals, water, and sodium bicarbonate in a laboratory simulation. The laboratory impact conditions correspond to a part of the terrestrial impacts on Hadean Earth that had oceans with  $CO_2$ - $N_2$ -rich atmosphere, although the duration of the temperature and pressure are significantly limited in this study. Therefore, Fe-bearing asteroid/meteorite impacts on Hadean Earth might have provided locally enriched FA, which is important for the scenario of the abiotic synthesis of the building blocks of life. This type of FA synthesis might also have been possible on Noachian Mars, given the presence of a  $CO_2$ - $N_2$  atmosphere and an ocean.

## Acknowledgments

The authors thank U. Takeuchi and N. Terada for the support in conducting experiments and in the discussion. This study was supported by funding from JSPS KAKENHI (T.K., 15H02144 and 18H03729), NINS Astrobiology Center satellite research (Y.F.), and the Tohoku University FRIS research program (T.K. and Y.F.).

## References

Abe, Y., and Matsui, T. (1988) Evolution of an impact-generated  $H_2O$ - $CO_2$  atmosphere and formation of a hot proto-ocean on Earth. *J Atmos Sci* 45:3081–3101.

- Anders, E. (1989) Pre-biotic organic-matter from comets and asteroids. *Nature* 342:255–257.
- Aponte, J.C., Whitaker, D., Powner, M.W., Elsila, J.E., and Dworkin, J.P. (2019) Analyses of aliphatic aldehydes and ketones in carbonaceous chondrites. *ACS Earth Space Chem* 3:463–472.
- Batalha, N., Domagal-Goldman, S.D., Ramirez, R., and Kasting, J.F. (2015) Testing the early Mars H<sub>2</sub>–CO<sub>2</sub> greenhouse hypothesis with a 1-D photochemical model. *Icarus* 258:337–349.
- Benner, S.A., Devine, K.G., Matveeva, L.N., and Powell, D.H. (2000) The missing organic molecules on Mars. *Proc Natl Acad Sci USA* 97:2425–2430.
- Benner, S.A., Bell, E.A., Biondi, E., Brasser, R., Carell, T., Kim, H.-J., Mojzsis, S.J., Omran, A., Pasek, M.A., and Trail, D. (2020) When did life likely emerge on Earth in an RNA-first process? *ChemSystemsChem* 2, doi:10.1002/syst.201900035.
- Bontemps, S., Vendier, L., and Sabo-Etienne, S. (2014) Ruthenium-catalyzed reduction of carbon dioxide to formaldehyde. *J Am Chem Soc* 136:4419–4425.
- Breslow, R. (1959) On the mechanism of the formose reaction. *Tetrahedron Lett* 1:22–26.
- Carr, M.H., and Head, J.W. (2010) Geologic history of Mars. *Earth Planet Sci Lett* 294:185–203.
- Chyba, C., and Sagan, C. (1992) Endogenous production, exogenous delivery and impact-shock synthesis of organic molecules: an inventory for the origins of life. *Nature* 355:125–132.
- Civiš, S., Szabla, R., Szyja, B.M., Smykowski, D., Ivanek, O., Knížek, A., Kubelík, P., Šponer, J., Ferus, M., and Šponer, J.E. (2016) TiO<sub>2</sub>-catalyzed synthesis of sugars from formaldehyde in extraterrestrial impacts on the early Earth. *Sci Rep* 6, doi:10.1038/srep23199.
- Cleaves, H.J. (2008) The prebiotic geochemistry of formaldehyde. *Precambrian Res* 164:111–118.
- Day, J.M.D., Brandon, A.D., and Walker, R.J. (2016) Highly siderophile elements in Earth, Mars, the Moon, and asteroids. *Rev Mineral Geochem* 81:161–238.
- Di Achille, G., and Hynek, B.M. (2010) Ancient ocean on Mars supported by global distribution of deltas and valleys. *Nat Geosci* 3:459–463.
- Ehlmann, B.L., Mustard, J.F., Murchie, S.L., Poulet, F., Bishop, J.L., Brown, A.J., Calvin, W.M., Clark, R.N., Des Marais, D.J., Milliken, R.E., Roach, L.H., Roush, T.L., Swayze, G.A., and Wray, J.J. (2008) Orbital identification of carbonate-bearing rocks on Mars. *Science* 322:1828–1832.
- Fairén, A.G., Dohm, J.M., Baker, V.R., de Pablo, M.A., Ruiz, J., Ferris, J.C., and Anderson, R.C. (2003) Episodic flood inundations of the northern plains of Mars. *Icarus* 165:53–67.
- Ferus, M., Nesvorný, D., Šponer, J., Kubelík, P., Michalčíková, R., Shestivská, V., Šponer, J.E., and Civiš, S. (2015) High-energy chemistry of formamide: a unified mechanism of nucleobase formation. *Proc Natl Acad Sci USA* 112:657–662.
- Ferus, M., Pietrucci, F., Saitta, A.M., Knížek, A., Kubelík, P., Ivanek, O., Shestivská, V., and Civiš, S. (2017) Formation of nucleobases in a Miller–Urey reducing atmosphere. *Proc Natl Acad Sci USA* 114:4306–4311.
- Ferus, M., Pietrucci, F., Saitta, A.M., Ivanek, O., Knížek, A., Kubelík, P., Krus, M., Juha, A., Dudzak, R., Dostál, J., Pastorek, A., Petera, L., Hrnčirova, J., Saeidifirozeh, H., Shestivská, V., Šponer, J., Šponer, J.E., Rimmer, P., Civiš, S., and Cassone, G. (2019) Prebiotic synthesis initiated in formaldehyde by laser plasma simulating high-velocity impacts. *Astron Astrophys* 626, doi:10.1051/0004-6361/201935435.
- Furukawa, Y., Nakazawa, H., Sekine, T., and Kakegawa, T. (2007) Formation of ultrafine particles from impact-generated supercritical water. *Earth Planet Sci Lett* 258:543–549.
- Furukawa, Y., Sekine, T., Oba, M., Kakegawa, T., and Nakazawa, H. (2009) Biomolecule formation by oceanic impacts on early Earth. *Nat Geosci* 2:62–66.
- Furukawa, Y., Sekine, T., Kakegawa, T., and Nakazawa, H. (2011) Impact-induced phyllosilicate formation from olivine and water. *Geochim Cosmochim Acta* 75:6461–6472.
- Furukawa, Y., Samejima, T., Nakazawa, H., and Kakegawa, T. (2014) Experimental investigation of reduced volatile formation by high-temperature interactions among meteorite constituent materials, water, and nitrogen. *Icarus* 231:77–82.
- Furukawa, Y., Nakazawa, H., Sekine, T., Kobayashi, T., and Kakegawa, T. (2015) Nucleobase and amino acid formation through impacts of meteorites on the early ocean. *Earth Planet Sci Lett* 429:216–222.
- Furukawa, Y., Chikaraishi, Y., Ohkouchi, N., Ogawa, N.O., Glavin, D.P., Dworkin, J.P., Abe, C., and Nakamura, T. (2019) Extraterrestrial ribose and other sugars in primitive meteorites. *Proc Natl Acad Sci USA* 116:24440–24445.
- Harada, K. (1963) Asymmetric synthesis of  $\alpha$ -amino-acids by Strecker synthesis. *Nature* 200, doi:10.1038/2001201a0.
- Hartmann, W.K., and Neukum, G. (2001) Cratering chronology and the evolution of Mars. *Space Sci Rev* 96:165–194.
- Hartmann, W.K., Ryder, G., Dones, L., and Grinspoon, D. (2000) The time-dependent intense bombardment of the primordial Earth/Moon system. In *Origin of the Earth and Moon*, edited by R.M. Canup and K. Righter, University of Arizona Press, Tucson, AZ, pp 493–512.
- Hashimoto, G.L., Abe, Y., and Sugita, S. (2007) The chemical composition of the early terrestrial atmosphere: formation of a reducing atmosphere from CI-like material. *J Geophys Res Planets* 112, doi:10.1029/2006JE002844.
- Head, J.W., Hiesinger, H., Ivanov, M.A., Kreslavsky, M.A., Pratt, S., and Thomson, B.J. (1999) Possible ancient oceans on Mars: evidence from Mars Orbiter Laser Altimeter data. *Science* 286:2134–2137.
- Hills, J.G., and Goda, M.P. (1993) The fragmentation of small asteroids in the atmosphere. *Astron J* 105:1114–1144.
- Holland, H.D. (1984) *The Chemical Evolution of the Atmosphere and Oceans*, Princeton University Press, Princeton, NJ.
- Idriss, H., Lusvardi, V.S., and Barteau, M.A. (1996) Two routes to formaldehyde from formic acid on TiO<sub>2</sub>(001) surfaces. *Surface Science* 348:39–48.
- Kasting, J.F. (1990) Bolide impacts and the oxidation state of carbon in the Earth's early atmosphere. *Orig Life Evol Biosph* 20:199–231.
- Kasting, J.F. (1993) Earth's early atmosphere. *Science* 259:920–926.
- Kim, H.-J., Ricardo, A., Illangkoon, H.I., Kim, M.J., Carrigan, M.A., Frye, F., and Benner, S.A. (2011) Synthesis of carbohydrates in mineral-guided prebiotic cycles. *J Am Chem Soc* 133:9457–9468.
- Kimura, M., Imae, N., Yamaguchi, A., Haramura, H., and Kojima, H. (2018) Bulk chemical compositions of Antarctic meteorites in the NIPR collection. *Polar Sci* 15:24–28.
- Korablev, O.I., Ackerman, M., Krasnopolsky, V.A., Moroz, V.I., Muller, C., Rodin, A.V., and Atreya, S.K. (1993) Tentative identification of formaldehyde in the martian atmosphere. *Planet Space Sci* 41:441–451.
- Kurosawa, K., Sugita, S., Ishibashi, K., Hasegawa, S., Sekine, Y., Ogawa, N., Kadono, T., Ohno, S., Ohkouchi, N., Nagaoka, Y., and Matsui, T. (2013) Hydrogen cyanide production due to

- mid-size impacts in a redox-neutral N<sub>2</sub>-rich atmosphere. *Orig Life Evol Biosph* 43:221–245.
- Miller, S.L. (1953) A production of amino acids under possible primitive Earth conditions. *Science* 117:528–529.
- Mittlefehldt, D.W., McCoy, T.J., Goodrich, C.A., and Kracher, A. (1998) Non-chondritic meteorites from asteroidal bodies. In *Planetary Materials*, edited by J.J. Papikes, De Gruyter, Boston, MA, pp D1–D195.
- Mukhin, L.M., Gerasimov, M.V., and Safonova, E.N. (1989) Origin of precursors of organic molecules during evaporation of meteorites and mafic terrestrial rocks. *Nature* 340: 46–48.
- Nakazawa, H. (2018) *Darwinian Evolution of Molecules*, Springer, Singapore.
- Nakazawa, H., Sekine, T., Kakegawa, T., and Nakazawa, S. (2005) High yield shock synthesis of ammonia from iron, water and nitrogen available on the early Earth. *Earth Planet Sci Lett* 235:356–360.
- Pasek, M., and Lauretta, D. (2008) Extraterrestrial flux of potentially prebiotic C, N, and P to the early Earth. *Orig Life Evol Biosph* 38:5–21.
- Pierazzo, E., and Chyba, C.F. (1999) Amino acid survival in large cometary impacts. *Meteorit Planet Sci* 34:909–918.
- Pierazzo, E., and Melosh, H.J. (2000) Hydrocode modeling of oblique impacts: the fate of the projectile. *Meteorit Planet Sci* 35:117–130.
- Pinto, J.P., Gladstone, G.R., and Yung, Y.L. (1980) Photochemical production of formaldehyde in Earth's primitive atmosphere. *Science* 210:183–184.
- Rotelli, L., Trigo-Rodríguez, J.M., Moyano-Camero, C.E., Carota, E., Botta, L., Di Mauro, E., and Saladino, R. (2016) The key role of meteorites in the formation of relevant prebiotic molecules in a formamide/water environment. *Sci Rep* 6, doi:10.1038/srep38888.
- Schaefer, L., and Fegley, B. (2010) Chemistry of atmospheres formed during accretion of the Earth and other terrestrial planets. *Icarus* 208:438–448.
- Schmidt, M.E., Schrader, C.M., and McCoy, T.J. (2013) The primary fO<sub>2</sub> of basalts examined by the Spirit rover in Gusev Crater, Mars: evidence for multiple redox states in the martian interior. *Earth Planet Sci Lett* 384:198–208.
- Sekine, T. (1997) Shock wave chemical synthesis. *European Journal of Solid State and Inorganic Chemistry* 34:823–833.
- Shimamura, K., Shimojo, F., Nakano, A., and Tanaka, S. (2016) Meteorite impact-induced rapid NH<sub>3</sub> production on early Earth: *ab initio* molecular dynamics simulation. *Sci Rep* 6, doi:10.1038/srep38953.
- Shimamura, K., Shimojo, F., Nakano, A., and Tanaka, S. (2019) *Ab initio* molecular dynamics study of prebiotic production processes of organic compounds at meteorite impacts on ocean. *J Comput Chem* 40:349–359.
- Squyres, S.W., Grotzinger, J.P., Arvidson, R.E., Bell, J.F., Calvin, W., Christensen, P.R., Clark, B.C., Crisp, J.A., Farrand, W.H., Herkenhoff, K.E., Johnson, J.R., Klingelhöfer, G., Knoll, A.H., McLennan, S.M., McSween, H.Y., Morris, R.V., Rice, J.W., Rieder, R., and Soderblom, L.A. (2004) *In situ* evidence for an ancient aqueous environment at Meridiani Planum, Mars. *Science* 306:1709–1714.
- Sugita, S., and Schultz, P.H. (2003) Interactions between impact-induced vapor clouds and the ambient atmosphere: 1. Spectroscopic observations using diatomic molecular emission. *J Geophys Res Planets* 108, doi:10.1029/2002JE001959.
- Summers, M.E., Lieb, B.J., Chapman, E., and Yung, Y.L. (2002) Atmospheric biomarkers of subsurface life on Mars. *Geophys Res Lett* 29:24-1–24-4.
- Takeuchi, Y., Furukawa, Y., Kobayashi, T., Sekine, T., Terada, N., and Kakegawa, T. (2020) Impact-induced amino acid formation on Hadean Earth and Noachian Mars. *Sci Rep* 10, doi:10.1038/s41598-020-66112-8.
- Tian, F., Toon, O.B., Pavlov, A.A., and De Sterck, H. (2005) A hydrogen-rich early Earth atmosphere. *Science* 308:1014–1017.
- Trail, D., Watson, E.B., and Tailby, N.D. (2011) The oxidation state of Hadean magmas and implications for early Earth's atmosphere. *Nature* 480:79–82.
- Valley, J.W., Peck, W.H., King, E.M., and Wilde, S.A. (2002) A cool early Earth. *Geology* 30:351–354.
- Weiss, B.P., Yung, Y.L., and Nealson, K.H. (2000) Atmospheric energy for subsurface life on Mars? *Proc Natl Acad Sci USA* 97:1395–1399.
- Yanagawa, H., Kobayashi, Y., and Egami, F. (1980) Genesis of amino acids in the primeval sea: formation of amino acids from sugars and ammonia in a modified sea medium. *J Biochem* 87:359–362.
- Yang, X., Gaillard, F., and Scaillet, B. (2014) A relatively reduced Hadean continental crust and implications for the early atmosphere and crustal rheology. *Earth Planet Sci Lett* 393: 210–219.

Address correspondence to:  
Yoshihiro Furukawa  
Department of Earth Science  
Tohoku University  
6-3 Aza-aoba, Aramaki, Aoba-ku  
Sendai 980-8578  
Japan

E-mail: furukawa@tohoku.ac.jp

Submitted 12 June 2020  
Accepted 9 November 2020  
Associate Editor: Nita Sahai

#### Abbreviations Used

CC = carbonaceous chondrite type  
DNPH = 2,4-dinitrophenylhydrazine  
FA = formaldehyde  
IM = iron meteorite type  
LHB = Late Heavy Bombardment  
MRM = multiple reaction monitoring  
OC = ordinary chondrite type  
UHPLC/MSMS = ultra-high-performance liquid chromatography/tandem mass spectrometry  
XRD = X-ray diffraction